

Keep Rehearsing and Refining: Lifelong Learning Vehicle Routing under Continually Drifting Tasks

Jiyuan Pei¹ Yi Mei¹ Jialin Liu² Mengjie Zhang¹ Xin Yao²

Abstract

Existing neural solvers for vehicle routing problems (VRPs) are typically trained either in a one-off manner on a fixed set of pre-defined tasks or in a lifelong manner on several tasks arriving sequentially, assuming sufficient training on each task. Both settings overlook a common real-world property: problem patterns may drift continually over time, yielding massive tasks sequentially arising while offering only limited training resources per task. In this paper, we study a novel lifelong learning paradigm for neural VRP solvers under continually drifting tasks over learning time steps, where sufficient training for any given task at any time is not available. We propose Dual Replay with Experience Enhancement (DREE), a general framework to improve learning efficiency and mitigate catastrophic forgetting under such drift. Extensive experiments show that, under such continual drift, DREE effectively learns new tasks, preserves prior knowledge, improves generalization to unseen tasks, and can be applied to diverse existing neural solvers.

1. Introduction

Although neural solvers for vehicle routing problems (VRP) have achieved impressive performance by leveraging the strong capability of deep learning (Kwon et al., 2020; Bengio et al., 2021; Bogrybayeva et al., 2024; Sun et al., 2024; Chen et al., 2025a; Huang et al., 2025), especially deep reinforcement learning (DRL), they are predominantly built upon a restrictive assumption: abundant training resources are available from each task (problem pattern) that is pre-defined and stationary. Training instances at all time steps during learning are independent and identically distributed,

¹Center of Data Science and Artificial Intelligence & School of Engineering and Computer Science, Victoria University of Wellington, Wellington, New Zealand. ²School of Data Science, Lingnan University, Hong Kong SAR, China.. Correspondence to: Yi Mei <yi.mei@ecs.vuw.ac.nz>.

Preprint. February 2, 2026.

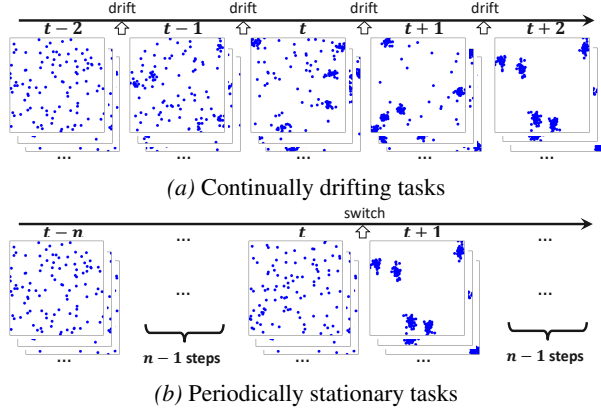


Figure 1. VRP instances arise in lifelong learning scenarios, with node distribution of the task changes from uniform to clustered.

assuming patterns/tasks remain unchanged during learning. However, real-world scenarios often depart from this stationary regime (Markov et al., 2020; Liu et al., 2021; Wang et al., 2024c; Mardešić et al., 2024; Li et al., 2025b). New VRP instances arise sequentially over time, while their underlying patterns often drift continually (cf. Figure 1a). For example, in daily urban delivery, a set of new routing problem instances arises for each new day, and the distribution of customer locations and traffic conditions changes continually over days due to the gradual population migration and urban construction. Meanwhile, previously encountered patterns may re-emerge due to unexpected stochastic factors (e.g., holidays, road restoration, power system fault), generating new instances with seen patterns. Under such a drift, one-off training becomes insufficient. Solvers trained for historical tasks tend to suffer performance degradation on newly emerging patterns (Sun et al., 2018; Zhang et al., 2023). This gap motivates the need for VRP solvers that can continue to learn from continually drifting tasks while maintaining competence on previously encountered tasks.

Some recent studies (Li et al., 2025a; Feng et al., 2025; Pei et al., 2025c) have begun exploring lifelong learning for neural VRP solvers, aiming to improve plasticity, i.e., the ability to learn new tasks, and stability, i.e., the ability to preserve knowledge of previously learned tasks and avoid catastrophic forgetting. However, their works mainly focus

on the particular scenario considering periodically stationary tasks with sufficient per-task learning (denoted *periodically stationary* scenario, cf. Figure 1b). Each task remains stationary for a long time interval (hundreds of training steps with millions of instances) to be learned before the arrival of the next task. Under this strong assumption, these methods typically rely on sufficient training for each stationary task and on storing high-quality task-specific knowledge, such as model parameters (Li et al., 2025a; Feng et al., 2025) or behaviors (Pei et al., 2025c) for transferring and mitigating forgetting. However, in real-world scenarios where the problem patterns drift continually, such assumptions no longer hold. Obtaining and storing high-quality per-task knowledge becomes impractical. As our experiments demonstrate (cf. Section 5.2), lifelong learning solvers designed for the periodically stationary scenario can suffer substantial performance degradation.

In this work, we study a novel paradigm and provide a formal formulation of lifelong learning for neural VRP solvers, where the task changes continually during learning, with sufficient per-task training not available (referred to as *continually drifting* scenario). We propose Dual Replay with Experience Enhancement (DREE), a general framework designed for effective lifelong learning under continual task drift. DREE buffers and replays encountered problem instances as well as the corresponding behaviors of the solver simultaneously (*rehearsing*), so as to preserve rich knowledge under insufficient per-task training and mitigate forgetting caused by learning over a large variety of tasks. In addition, DREE proactively enhances the quality of buffered experiences through interactions between the two replay mechanisms (*refining*), addressing the misleading issue from low-quality experiences induced by insufficient per-task training. Comprehensive experimental studies on capacitated vehicle routing problems (CVRP) and traveling salesman problems (TSP) verify that DREE outperforms existing lifelong learning neural VRP methods in the continually drifting scenarios and has good applicability to different existing solvers.

Our main contributions are: (i) we introduce a novel paradigm with a formal formulation of lifelong learning with continual task drifting for neural VRP; (ii) we propose DREE, featuring novel dual replay and experience enhancement mechanisms tailored for this paradigm; and (iii) we verify the effectiveness of DREE through extensive experiments, comprehensive evaluation metrics, and detailed analysis.

2. Related Work

2.1. Neural VRP Solvers

By acquiring knowledge automatically from problem-solving experience, recent neural solvers lessen the dependence on human effort while achieving high problem-solving

performance (Bengio et al., 2021; Liu et al., 2023; Tang & Yao, 2024; Bogyrbayeva et al., 2024). Two types of neural solvers exist, i.e., construction and improvement (Bi et al., 2022; Kong et al., 2024). Construction neural solvers (e.g., (Kool et al., 2019; Kwon et al., 2020; Huang et al., 2025)) generate routes from scratch by choosing the next node step by step in an autoregressive process, and they can return strong solutions within seconds. Improvement neural solvers instead begin with a complete solution and refine it through repeated updates, for example, by learning how to configure (Wu et al., 2022; Ma et al., 2023) or how to choose among predefined improvement operators (Pei et al., 2025b; Chen et al., 2025b; Guo et al., 2025). In this work, we primarily study constructive neural solvers due to their broad applicability.

Existing neural VRP solvers typically rely on sufficient training in a one-off manner with hundreds of epochs and millions of training instances sampled from a pre-defined, stationary task (Kwon et al., 2020; Fang et al., 2024). After training, model parameters are frozen and directly applied to solve unseen instances. A key challenge is generalization (Gao et al., 2024; Zhou et al., 2025a). While these solvers often perform well on unseen instances i.i.d. to training ones, their performance degrades sharply on out-of-distribution instances drawn from unseen tasks (Jiang et al., 2022; 2023; Zhou et al., 2023; Liu et al., 2023). New model architectures (e.g., (Wang et al., 2024d; Xiao et al., 2025; Fang et al., 2024; Zheng et al., 2025)) and learning strategies (e.g., (Wang et al., 2024a; Liu et al., 2024a; Chen et al., 2025c)) are developed to improve generalization across tasks, yet they still rely on a representative pre-defined training task set and sufficient one-off learning on them, without actively reacting to potential arising new tasks.

2.2. Lifelong Learning Neural VRP Solvers

Fine-tuning is the standard approach when new tasks arise, namely training a solver pretrained on earlier tasks using instances from the new task (Zhou et al., 2023; Lin et al., 2024; Drakulic et al., 2025). However, fine-tuning leads to catastrophic forgetting, where parameters are overwritten to optimize the new task and performance drops substantially on previously learned tasks (Khetarpal et al., 2022; Wang et al., 2024b; Pei et al., 2025c). To better balance and improve plasticity for acquiring new tasks and stability for retaining prior knowledge, recent work has begun to study lifelong learning for neural VRP solvers in settings where training tasks arise sequentially (Li et al., 2025a; Feng et al., 2025; Pei et al., 2025c).

Buffering and replaying representative signals is an effective and widely adopted strategy for combating environmental drift (Rosin & Belew, 1997; Isele & Cosgun, 2018; Buzzega et al., 2020). All existing lifelong learning solvers (Li et al.,

2025a; Feng et al., 2025; Pei et al., 2025c) take experience replay as a key mechanism to mitigate catastrophic forgetting and facilitate knowledge transfer, but they differ in how experience is defined and replayed. Li et al. (2025a) and Feng et al. (2025) formulate problem instances as experience, assuming that the generation of new instances is controllable, and generate new instances of previous tasks to relearn old tasks during learning a new task. Sufficient trained model for each previous task is also utilized to guide later learning on a new task. In contrast, LLR-BC (Pei et al., 2025c) regards solver behaviors as experience. By storing high-quality solution trajectories generated when learning previous tasks and encouraging the model to imitate these preserved behaviors during subsequent task learning, LLR-BC demonstrates strong plasticity, stability, and generalization when tasks vary significantly in both scale and distribution.

Despite this progress, existing lifelong learning studies for neural VRP solver assume periodical stationary task. Their methods rely on sufficient per-task training, and obtaining high-quality task-specific models (Li et al., 2025a; Feng et al., 2025) or behaviors (Pei et al., 2025c) for subsequent knowledge consolidation. Issues arise in the continually drifting scenario. (i) A large number of tasks exist, each with highly limited training resources, making task-specific knowledge scarce and valuable. Using only instances or only behaviors as experience discards complementary information contained in the other. (ii) Without sufficient per-task training, the quality of buffered experience is substantially low. As a result, existing lifelong learning neural solvers are ineffective under the continually drifting scenario (cf. Section 5.2).

3. Lifelong Learning under Continually Drifting VRP Tasks

3.1. Continually Drifting VRP Task

A VRP task P can be defined as an instance-generating distribution in fixed settings, such as the problem scale (Liu et al., 2024b; Li et al., 2025a), the node-coordinate distribution (Jiang et al., 2023; Pei et al., 2025c), the set of constraints (Zhou et al., 2024; Pan et al., 2025; Luo et al., 2025), and the distance measurement (Feng et al., 2025).

Real-world deployments often exhibit continual task drift driven by evolving factors such as business growth (Markov et al., 2020; Mardešić et al., 2024; Li et al., 2025b). Under a fine-grained time discretization, the task can be approximately stationary within a single step, yet two consecutive steps are governed by related but different tasks. Reflecting practical cases, in the continually drifting lifelong learning scenario, multiple different tasks arrive sequentially over time. Specifically, training of totally T time steps is conducted on a sequence of tasks $\{P_1, \dots, P_T\}$, where

$P_t \neq P_{t'}, \forall t \neq t'$. Training at each step on the corresponding task is inherently insufficient, since neural solvers typically require a large number of steps to learn a single stationary task sufficiently (Kwon et al., 2020; Fang et al., 2024; Li et al., 2025a; Feng et al., 2025).

The periodically stationary scenario studied by existing works (Li et al., 2025a; Feng et al., 2025; Pei et al., 2025c) assumes each task remains unchanged for n learning steps before the time step t that the next task arrives, i.e., $P_{t'} = P_t, \forall t' \in \{t-n, \dots, t-1\}$, where $n \gg 1$ so that sufficient per-task training is available. Compared with the periodically stationary scenario, the continually drifting scenario departs in that (i) no sufficient per-task training is guaranteed, and (ii) task distributions drift continuously over time steps rather than remaining constant over long intervals.

While plasticity is essential for adapting to new tasks, stability is also important. A solver should preserve performance on earlier tasks, as instances of them may re-occur and newly encountered tasks could be near-variants of past ones. The overall goal in the continual drifting scenario is to learn a solver that can produce high-quality solutions for instances drawn from any seen task of any time step.

3.2. Problem Formulation

We formally formulate lifelong learning in the continually drifting scenario as lifelong reinforcement learning.

A constructive neural solver operates on a VRP instance p by sequentially extending a partial solution, which can be modeled as a stationary instance-conditioned Markov decision process (MDP). Specifically, for an instance p , we define $\mathcal{M}(p) = \langle \mathcal{S}(p), \mathcal{A}(p), \mathcal{R}(p), \mathcal{T}(p) \rangle$, where a state s from the state space $\mathcal{S}(p)$ encodes p together with the current partial solution, an action a from the action space $\mathcal{A}(p)$ selects the ID of the next node to visit. The reward function $\mathcal{R}(p)$ is derived from the optimization objective (e.g., negative tour length (Kwon et al., 2020)). $\mathcal{T}(p)$ specifies the state transition under the instance-dependent constraints.

A training instance p is sampled from the task P_t at time step t , i.e., $p \sim P_t$. We consider only node characteristics changing between instances of a task, leading to different state spaces but identical action space, reward function and transition dynamics for different instances, i.e., $\mathcal{S}(p) \neq \mathcal{S}(p')$, $\mathcal{A}(p) = \mathcal{A}(p')$, $\mathcal{R}(p) = \mathcal{R}(p')$, $\mathcal{T}(p) = \mathcal{T}(p')$, $\forall p, p' \sim P_t$ and $p \neq p'$. As an instance forms an MDP, a task P_t introduces a distribution \mathbf{D}_t over the MDP, i.e., $\mathcal{M}(p) \sim \mathbf{D}_t$.

The distributions of MDP are different at different time steps, i.e., $\mathbf{D}_t \neq \mathbf{D}_{t'}, \forall t \neq t'$. Changing the distance measure (Feng et al., 2025) or the objective functions (Chen et al., 2025a) changes the reward function, while changing constraints (Lin et al., 2024; Zhou et al., 2025b) (resulting in different variants of the problem) modifies the transition

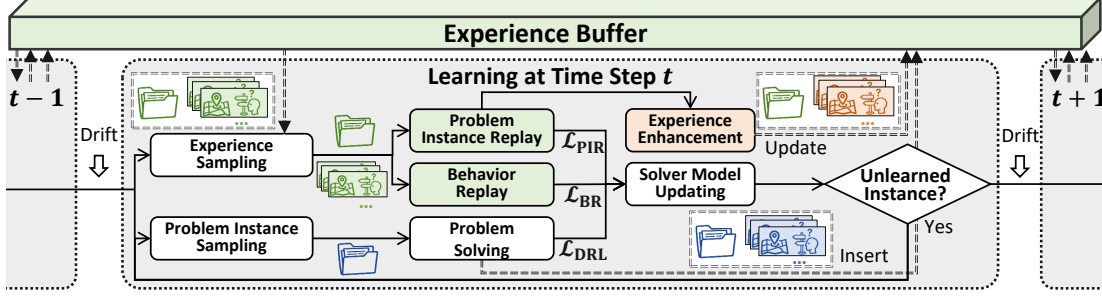


Figure 2. DREE in the lifelong learning scenario where the task drifts between every two consecutive time steps.

dynamics. In this work, we focus on drift in the problem scale and node distribution (Pei et al., 2025c). Consequently, distributions of $\mathcal{A}(p)$ and $\mathcal{S}(p)$ vary with t .

4. DREE

Experience replay of high-quality knowledge from previously seen tasks is a standard and effective strategy (Li et al., 2025a; Feng et al., 2025; Pei et al., 2025c) to mitigate catastrophic forgetting and promote knowledge transfer in lifelong learning scenarios. A good replay mechanism hinges on (i) what information is worth replaying as the experience, and (ii) how to obtain experience as high-quality as possible.

To effectively and efficiently learn in the continually drifting scenario, we propose **DREE** (cf. Figure 2), a general lifelong learning framework with three key mechanisms: *problem instance replay* (PIR), *behavior replay* (BR), and *experience enhancement* (EE). Since per-task knowledge is scarce and valuable, DREE buffers both problem instances and the solver’s behaviors on these instances as experiences, to preserve rich knowledge. During learning on a new task, DREE performs replay at both the instance level and behavior level to achieve effective knowledge consolidation. PIR enables the current solver to re-learn the buffered instances, reinforcing performance on past tasks. In parallel, BR regularizes learning by encouraging the solver to preserve high-quality behaviors on previous tasks, thereby transferring knowledge and reducing forgetting. To address the misleading of low-quality experiences, DREE actively improves the quality of buffered experiences. When the solver discovers a better solution for a buffered instance during PIR, the EE mechanism updates the stored behavior accordingly, continuously improving the quality of experiences. The following subsections introduce DREE’s key components. Appendix A provides more details.

4.1. Experience Buffer

The base neural solver conducts the learning of an instance $p \sim P_t$ of a task P_t to improve the performance on the task, by minimizing a loss $\mathcal{L}_{\text{DRL}}(\theta, p)$, where θ represents

the solver model. The definition of $\mathcal{L}_{\text{DRL}}(\theta, p)$ depends on the specific base solver used, and for different base solvers, the definition could be different. Experiences are generated while the solver learns the current task.

Each experience is defined as $e = \langle p, f, [(s, \pi)] \rangle$, where p denotes the problem instance, f is the objective value of a solution of p , and $[(s, \pi)]$ represents the corresponding solution construction trajectory, i.e., a sequence of states s and the solver’s action distributions (behaviors) π on them.

DREE maintains a buffer with a fixed size $|\mathcal{B}|$ and inserts newly generated experiences using reservoir sampling (Vitter, 1985), so that each seen experience has an equal probability of being retained. Specifically, a new experience is inserted directly if the memory is not full. Otherwise, each new experience replaces a randomly selected buffered experience with probability $\frac{|\mathcal{B}|}{|E|}$, where $|E|$ denotes the total number of new experiences generated so far.

As common practice, DREE trains with the problem instance in batch. Accordingly, experiences are also buffered and sampled at the batch level. During learning a new task, DREE obtains new instance batches of the new task, and randomly samples experience batches from the buffer for PIR and BR after learning each new instance batch.

Instead of fixing the experiences once buffered (Isele & Cosgun, 2018; Buzzega et al., 2020; Pei et al., 2025c), DREE actively updates them over time (cf. Section 4.4) to pursue higher-quality knowledge.

4.2. Problem Instance Replay

A direct way to improve performance on previous tasks is to solve and learn instances of them again, analogous to training on new-task instances. Prior works typically implement such replay by generating instances from previous task distributions during learning the new task (Li et al., 2025a; Feng et al., 2025). In contrast, DREE reuses the buffered instances, making it applicable even when instance generation is uncontrollable.

Specifically, for a buffered instance p_b , DREE re-solves it

using the current solver to obtain a new trajectory $[(s_\theta, \pi_\theta)]$ and a new solution with a new objective value $f(\theta, p_b)$. The base solver then applies its standard training objective on this trajectory, yielding a problem instance replay (PIR) loss

$$\mathcal{L}_{\text{PIR}}(\theta, e) = \mathcal{L}_{\text{DRL}}(\theta, p_b),$$

where p_b is the buffered problem instance in e . DREE performs PIR with an adaptive interval N , to balance plasticity and stability. For a batch of M replayed instances, let M^+ be the number of instances where the new objective is better than the buffered one. DREE schedules the next PIR after learning $N \leftarrow \text{UB} - \frac{M^+}{M} (\text{UB} - \text{LB})$ batches of new-task instances, where LB and UB are hyperparameters. Intuitively, a smaller $\frac{M^+}{M}$ indicates less potential to improve on previous tasks, triggering less frequent replay (larger N). $\mathcal{L}_{\text{PIR}}(\theta, e) \leftarrow 0$ when PIR is not performed.

4.3. Behavior Replay

For constructive solvers, the solution and its quality are fully determined by the construction behaviors. Thus, encouraging the solver to produce similar behaviors on the same (buffered) states is an effective and efficient way to preserve performance on previously learned tasks (Isele & Cosgun, 2018; Buzzega et al., 2020; Pei et al., 2025c).

To achieve this, the behavior replay (BR) introduces an additional loss term, $\mathcal{L}_{\text{BR}}(\theta, e)$, which measures the discrepancy between the buffered behaviors and those produced by the current solver. By minimizing $\mathcal{L}_{\text{BR}}(\theta, e)$, DREE mitigates catastrophic forgetting when learning new tasks.

Specifically, we conduct a problem instance-level behavior consolidation (Pei et al., 2025c) based on our experience definition, and define the behavior replay loss based on a buffered experience e as

$$\mathcal{L}_{\text{BR}}(\theta, e) = \sum_{s_b \in e} \bar{w}_e(s_b) \sum_{a \in \mathcal{A}} \pi_\theta(a \mid s_b) \log \frac{\pi_\theta(a \mid s_b)}{\pi_b(a \mid s_b)},$$

where $\pi_\theta(\cdot \mid s_b)$ is the current solver’s action distribution at a buffered state $s_b \in e$, $\pi_b(\cdot \mid s_b)$ is the buffered behavior stored in e corresponding to s_b , \mathcal{A} is the corresponding action space, and $\bar{w}_e(s_b)$ is a confidence-based weight computed by CaEW (Pei et al., 2025c).

4.4. Experience Enhancement

Behavior replay is effective when the target behaviors are of high quality, i.e., they correspond to solutions with good objective values (Pei et al., 2025c). In lifelong learning of VRP solvers, buffering behaviors only after sufficiently long training on a stationary task can ensure high-quality experiences (Pei et al., 2025c). However, in the continually drifting scenario, sufficient immediate per-task training is unavailable, leading to low-quality generated and buffered

experiences. Since behavior replay encourages imitation of buffered behaviors, low-quality targets may misguide learning and hurt lifelong performance.

PIR provides an opportunity to improve buffered behavior quality after experiences have been buffered. Solving the buffered instances with the current solver produces new solutions and trajectories whose objectives are directly comparable with the buffered ones. We thus introduce an *experience enhancement* mechanism. After performing PIR on a buffered batch, DREE compares the new objective $f(\theta, p)$ with the buffered objective f_b for each instance. Whenever $f(\theta, p)$ is better, i.e., $f(\theta, p) < f_b$, DREE updates the objective and the stored sequence of state-behavior pair with the newly generated sequence, i.e., $f_b \leftarrow f(\theta, p)$ and $[(s_b, \pi_b)] \leftarrow [(s_\theta, \pi_\theta)]$. As a result, BR always consolidates knowledge toward the best-so-far solutions and corresponding behaviors for each buffered instance, preserving the best performance on past tasks.

Overall, DREE optimizes the loss:

$$\mathcal{L}(\theta, p, e) = \mathcal{L}_{\text{DRL}}(\theta, p) + \alpha \mathcal{L}_{\text{BR}}(\theta, e) + \beta \mathcal{L}_{\text{PIR}}(\theta, e),$$

where θ is the current solver, $p \sim P_t$ is a training instances of the current task P_t , and e is the experience sampled from the buffer. α and β are hyperparameters.

5. Experiments

Focusing on continual drift lifelong learning scenarios of neural VRP solvers, we conduct comprehensive experimental studies to answer the following research questions:

- **Effectiveness:** Can DREE effectively and efficiently solve problem instances from learned tasks?
- **Stability and plasticity:** How does DREE perform in terms of stability and plasticity during learning?
- **Generalization:** Can DREE effectively solve problem instances from unseen tasks from different distributions and scales?
- **Hyperparameter sensitivity:** How sensitive is DREE to key hyperparameters: buffer size $|\mathcal{B}|$, the coefficients α and β in the loss function, and the PIR interval range defined by LB, UB?
- **Applicability:** Can DREE also work effectively in the periodically stationary scenario? And, can DREE work effectively on different base neural solvers?

We implement DREE with POMO (Kwon et al., 2020) as the base neural solver, given its concise design and broad applicability. Notably, DREE is a general framework and can be applied to a wide range of existing solvers.

5.1. Experimental Setups

Dataset. To our best knowledge, there is no available dataset tailored to the continually drifting lifelong learning scenario. We therefore construct a dataset based on the existing one designed for the periodically stationary scenario (Pei et al., 2025c). For both TSP and CVRP, we consider five random orders over six principal tasks ($P^U, P^R, P^{GM}, P^E, P^C, P^G$) with different node distributions and scales. We take an epoch (totally T epochs) as the unit of time steps (which is small enough, cf. Appendix B.1) and assign K predefined principal tasks $\{P^i\}_{i=1}^K$ evenly to K epochs with interval of $m = \frac{T}{K-1}$ epochs, i.e., to epochs $0, m, 2m, \dots, T$. The task of an epoch between the epochs of two principal tasks is a linear mixture of them. Specifically, an epoch $t \in \{im + 1, \dots, (i + 1)m - 1\}$, we generate an intermediate task P_t with scale $S_t = \left\lceil \frac{(i+1)m-t}{m} S^i + \frac{t-im}{m} S^{i+1} \right\rceil$, with S^i and S^{i+1} as the problem scales of P^i and P^{i+1} , respectively. For an instance of P_t , $\left\lceil \frac{t-im}{m} S_t \right\rceil$ nodes are generated with the distribution of P^{i+1} while the rest are generated with the distribution of P^i . Appendix B.1 provides more details. In addition, TSPLIB (Reinelt, 1991) and CVRPLIB (Uchoa et al., 2017), are used for generalization ability evaluation.

Training and Test Setting. Hyperparameters are set as follows: $|\mathcal{B}| = 256$, $\alpha = 100$ and $\beta = 1$, where $|\mathcal{B}|$ are defined in units of batches. During training, an epoch is the unit of time step. All instances generated in one epoch are i.i.d.. Training instances are sampled on the fly. We use a batch size of $M = 32$, train 128 batches per epoch, and $T = 1000$ epochs. Thus, each stationary task has 4,096 training instances, which is significantly less than a set of millions of instances used in existing studies for learning each task (Kwon et al., 2020; Pei et al., 2025c). Although the total number of training instances is the same, DREE involves additional problem-solving episodes due to PIR. For a fair comparison, we allow other lifelong learning methods to run more batches per epoch, ensuring that they perform the same number of episodes as DREE. For evaluation over different task orders, without loss of generality, we test the solver on the test instance set of each principal task, as principal tasks are consistent between orders, while intermediate tasks are not. Each principal task has 1000 test instances, which are consistent for all compared methods and task orders. Additional details are provided in Appendix B.2.

Comparison Methods. First, we include the commonly applied strategy in neural solver studies (Kwon et al., 2020; Zhou et al., 2023), *fine-tuning*, which sequentially trains the solver only on the current task at each time step. We then adapt existing lifelong-learning neural VRP solvers, which are all designed for the periodically stationary scenario, to the continually drifting scenario, including (ii) the method

of Li et al. (2025a) (denoted *Li*) and (iii) LLR-BC (Pei et al., 2025c). We also evaluate (iv) a multi-task setting, *MT-Ref*, which has access to all possible tasks and samples training instances by randomly switching t in each batch (Pei et al., 2025c). Notably, *MT-Ref* only serves as an idealized reference, it is not practically applicable in lifelong learning scenarios. We exclude other methods compared by Pei et al. (2025c) (e.g., methods of Pei et al. (2025a); Feng et al. (2025)), as they store one solver per task and repeatedly compare against all stored solvers. This is prohibitively expensive in continually drifting, where massive stationary tasks are encountered over time. Appendix B.3 presents more details about the adaptation and method settings.

Evaluation Metrics. We evaluate a lifelong learning solver with a comprehensive set of metrics, adapted from metrics designed for the periodically stationary scenario (Pei et al., 2025c). Let $d_{t,i}$ denote the *test performance*, i.e., average optimality gap (%) over all the test instances, of the solver on principal task P_i after t th training epoch. d_i^* denotes the best (smallest) obtained test performance on a principal task P^i in one lifelong learning process, and t_i^* denotes the epoch that d_i^* is achieved (i.e., $d_i^* = d_{t_i^*,i}$). Based on this notation, after all T epochs of one lifelong learning, we calculate (smaller is better for all):

- **Average Performance (AP):** the current average performance on tasks learned, i.e., $AP = \frac{1}{K} \sum_{i=1}^K d_{E,i}$.
- **Average Forgetting after Best (AFB):** the average performance decrease on previously learned tasks after the best performance of this task is achieved, i.e., $AFB = \frac{1}{K} \sum_{i=1}^K d_{E,i} - d_i^*$.
- **Average Max Forgetting after Best (AMFB):** the average of maximal forgetting of each learned task during the lifelong learning, i.e., $AMFB = \frac{1}{K} \sum_{i=1}^K \max_{t=e_i^*}^E d_{t,i} - d_i^*$.
- **Average Best Plasticity (ABPl):** the average of best performance a solver achieves on each task, i.e., $ABPl = \frac{1}{K} \sum_{i=1}^K d_i^*$.

5.2. Performance Analysis

Performances on Seen Tasks. Table 1 demonstrates the metrics of each method. In terms of AP, DREE stably (with the smallest std.) outperforms (with a smaller mean) all compared lifelong learning methods over task orders on both TSP and CVRP. DREE even performs closely to *MT-Ref*, which can access all tasks simultaneously. It verifies DREE’s effectiveness in solving tasks after lifelong learning of them.

Plasticity during Learning. As shown in Table 1, DREE attains the smallest ABPl on CVRP and the second smallest

Table 1. Mean (std.) over five task orders. MT-Ref is trained jointly on all possible tasks (not lifelong learning), thus ABPI/AFB/MBF are not applicable. MT-Ref is task-order invariant and is run once (no std.).

Method	CVRP				TSP			
	AP	AFB	AMFB	ABPI	AP	AFB	AMFB	ABPI
MT-Ref	3.04	-	-	-	0.91	-	-	-
Fine-tuning	8.75 (4.40)	5.47 (4.27)	15.75 (6.13)	3.28 (0.29)	1.97 (0.30)	0.86 (0.07)	1.64 (0.32)	1.11 (0.28)
Li	6.16 (0.38)	0.09 (0.06)	0.10 (0.06)	6.07 (0.38)	4.43 (0.96)	0.02 (0.01)	0.05 (0.05)	4.42 (0.95)
LLR-BC	4.19 (0.32)	1.10 (0.19)	1.76 (0.18)	3.09 (0.28)	1.36 (0.32)	0.17 (0.08)	0.32 (0.18)	1.19 (0.27)
DREE	3.11 (0.13)	0.23 (0.15)	0.42 (0.34)	2.88 (0.12)	1.21 (0.26)	0.06 (0.04)	0.08 (0.04)	1.16 (0.27)

on TSP, indicating strong plasticity. This suggests that the BC, IR, and EE mechanisms effectively transfer knowledge from previous tasks to facilitate learning on new tasks.

Stability during Learning. As shown in Table 1, *fine-tuning* exhibits severe forgetting (large AFB and AMFB), as expected. *Li* strongly biases toward stability, yielding very small forgetting but substantially sacrificing plasticity (large AP and ABPI). In contrast, while maintaining promising plasticity, DREE achieves lower forgetting than all compared methods except *Li* for both TSP and CVRP in terms of AFB and AMFB, highlighting the effectiveness of the key modules of DREE (BC, IR, and EE) in mitigating forgetting. We record the solver after each epoch, and Figure 3 shows their test performance. DREE effectively improves performance on new tasks while stably preserving, sometimes even improving, its performance on previously learned tasks.

Performances on Unseen Benchmark Instances. Table 2 lists the test performance of solvers obtained from lifelong learning on task order 1 on CVRPLIB and TSPLIB. DREE outperforms (smaller gap) all compared lifelong learning methods on both benchmarks and obtains close (TSP) or even better (CVRP) performance as *MT-Ref*, verifying its promising generalization ability by capturing general knowledge across tasks. Appendix C.2 presents more details.

Table 2. Mean (Std.) optimality gap on benchmark instances.

Method	CVRPLIB	TSPLIB
MT-Ref	12.92 (4.90)	19.86 (10.69)
Fine-tuning	16.32 (6.39)	19.74 (9.56)
Li	21.66 (7.13)	30.20 (13.76)
LLR-BC	35.57 (31.83)	18.91 (9.60)
DREE	13.78 (6.40)	18.77 (9.46)

5.3. Applicability

To periodically stationary scenario. We further compare DREE with *fine-tuning* and LLR-BC under the periodically stationary scenario (Pei et al., 2025c) with task order 1. We do not include the methods of Li et al. (2025a) and Feng et al.

(2025), since LLR-BC has been shown to outperform them in this scenario (Pei et al., 2025c). As reported in Table 3, DREE achieves performance comparable to LLR-BC, the state-of-the-art for the periodically stationary scenario, and is even slightly better on CVRP. These results confirm DREE’s strong applicability to different scenarios.

Table 3. Metrics on the periodically stationary scenario.

Method	CVRP				TSP			
	AP	AFB	AMFB	ABPI	AP	AFB	AMFB	ABPI
Fine-tuning	6.67	4.34	6.44	2.34	2.40	1.68	4.13	0.73
LLR-BC	2.55	0.28	0.31	2.27	0.70	0.07	0.16	0.63
DREE	2.30	0.04	0.09	2.26	0.72	0.05	0.21	0.67

To Different Based Solvers. To verify that the superior performance of DREE over other lifelong learning solver does not stem from a bias toward a specific base solver (e.g., POMO), we conduct a comparison based on two other existing solvers (i.e., Omni (Zhou et al., 2023) and INViT (Fang et al., 2024)), following Pei et al. (2025c). We implement and compare DREE with *fine-tuning* and LLR-BC on task order 1. Our goal is not to compare across base solvers but to evaluate different lifelong learning methods on the same base solver. The results across different base solvers are not directly comparable, as training settings are different (cf. Appendix C.3). As Table 4 shows, DREE outperforms *fine-tuning* and LLR-BC generally, with a similar pattern found on POMO. In summary, DREE is effective in the continually drafting scenario, without relying on specific characteristics of the base solver.

Table 4. Metric values with Omni or INViT as the base solver.

Method	CVRP				TSP			
	AP	AFB	AMFB	ABPI	AP	AFB	AMFB	ABPI
Fine-tuning (INViT)	24.65	0.67	0.84	23.98	12.65	0.25	0.41	12.40
LLR-BC (INViT)	23.83	0.33	0.66	23.49	11.78	0.25	0.62	11.54
DREE (INViT)	21.93	0.24	0.56	21.69	10.99	0.16	0.21	10.83
Fine-tuning (Omni)	5.67	2.46	7.63	3.20	1.02	0.31	1.04	0.71
LLR-BC (Omni)	3.98	1.07	2.52	2.91	1.08	0.07	0.09	1.01
DREE (Omni)	3.45	0.54	1.52	2.91	0.98	0.06	0.07	0.93

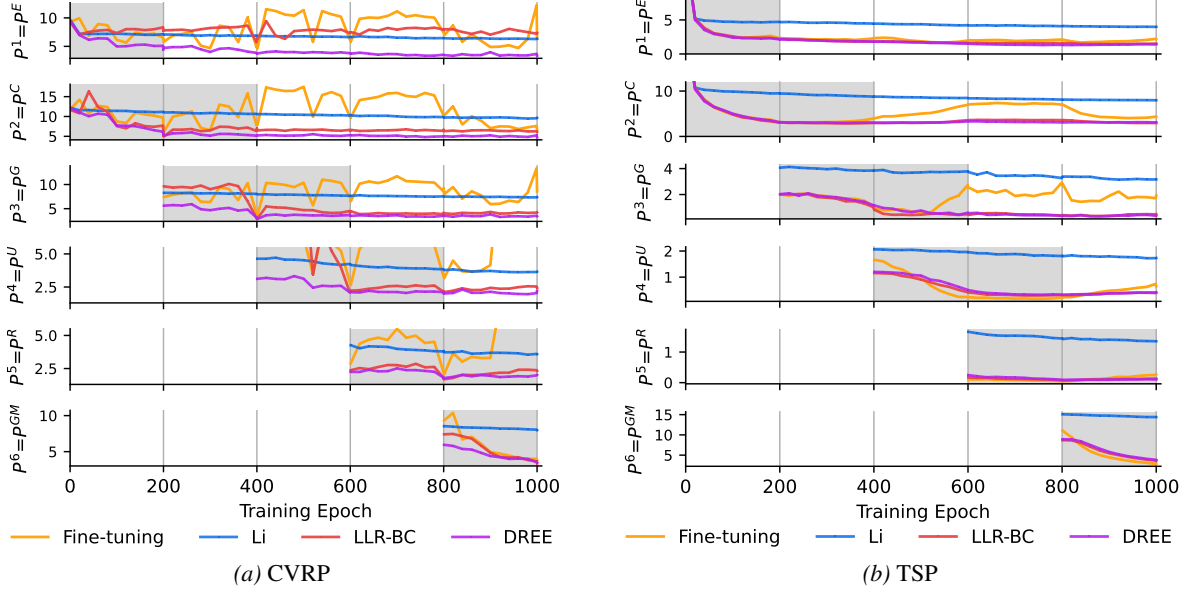


Figure 3. Learning curve of task order 1, measured by test performance. Grey background indicates the epochs that the corresponding principal task is involved in generating intermediate tasks.

5.4. Ablation Study and Hyperparameter Analysis

Comparison with Ablation Versions. We form ablation versions by removing PIR, BR, and EE individually, denoted as $nPIR$, nBR , and nEE , respectively. More details are in Appendix C.4. We run them on task order 1, and Table 5 lists the results. Removing each key component leads to performance degradation across multiple metrics on both CVRP and TSP, confirming the contribution of each module.

Comparison between Different Hyperparameter Settings. We vary the values of key hyperparameters and evaluate DREE under each setting, as reported in Table 5. Additional details are provided in Appendix C.5. We denote a variant with hyperparameter k set to v as $k(v)$. Overall, varying these hyperparameters causes only minor fluctuations across metrics, considering the performance gap between DREE and the baselines. This suggests that DREE is not overly sensitive to its hyperparameter settings.

6. Conclusions

In this work, we study lifelong learning for neural VRP solvers under continual task drift, and formulate it as a lifelong RL problem with a drifting MDP distribution. We propose DREE, which integrates problem instance replay, behavior replay, and experience enhancement to continually acquire, rehearse, and refine experience. Empirically, DREE achieves superior performance to existing lifelong learning solvers under the continually drifting scenario, while remaining competitive on the periodically stationary scenario studied by prior works. These results highlight that,

Table 5. Metrics of DREE in different settings, on task order 1.

Method	CVRP				TSP			
	AP	AFB	AMFB	ABPI	AP	AFB	AMFB	ABPI
nPIR	4.07	0.81	2.23	3.25	1.32	0.12	0.20	1.20
nBR	3.87	0.53	1.70	3.33	1.34	0.29	0.48	1.06
nEE	3.47	0.32	0.49	3.16	1.30	0.14	0.21	1.16
$\alpha(50)$	3.34	0.46	1.48	3.48	1.08	0.08	0.14	1.01
$\alpha(200)$	3.25	0.28	0.36	2.97	1.37	0.05	0.07	1.31
$\beta(0.5)$	3.27	0.23	0.79	3.04	1.22	0.08	0.12	1.14
$\beta(2)$	3.13	0.16	0.30	2.97	1.22	0.05	0.06	1.16
$ \mathcal{B} (128)$	3.19	0.27	0.43	2.92	1.19	0.06	0.09	1.13
$ \mathcal{B} (64)$	3.24	0.29	0.35	2.96	1.22	0.12	0.13	1.10
UB(8)	3.30	0.24	0.63	3.06	1.26	0.14	0.15	1.13
LB(2)	3.14	0.24	0.38	2.90	1.19	0.05	0.08	1.14
DREE	3.16	0.22	0.42	2.94	1.11	0.07	0.09	1.04

in lifelong learning of VRP solvers, both problem instances and behaviors constitute critical experience, and enhancing the quality of buffered experience is crucial for effective replay-based lifelong learning.

Despite its strong results, DREE treats tasks from all time steps equally. A potential future direction is to selectively emphasize steps that accumulate significant drift and are most distinctive to others, which may further improve learning efficiency. Incorporating strategies from dynamic optimization (Yang, 2015) or online learning (Zhang et al., 2023) has potential for performance improvement. Extending DREE to scenarios with continually drifting constraints, so as to lifelong learn diverse problem variants, also constitutes a promising future direction.

References

- Bengio, Y., Lodi, A., and Prouvost, A. Machine learning for combinatorial optimization: A methodological tour d’horizon. *European Journal of Operational Research*, 290(2):405–421, 2021.
- Bi, J., Ma, Y., Wang, J., Cao, Z., Chen, J., Sun, Y., and Chee, Y. M. Learning generalizable models for vehicle routing problems via knowledge distillation. In *NeurIPS*, volume 35, pp. 31226–31238, 2022.
- Bogyrbayeva, A., Meraliyev, M., Mustakhov, T., and Dauletbayev, B. Machine learning to solve vehicle routing problems: A survey. *IEEE Transactions on Intelligent Transportation Systems*, 25(6):4754–4772, 2024.
- Buzzega, P., Boschini, M., Porrello, A., Abati, D., and Calderara, S. Dark experience for general continual learning: A strong, simple baseline. In *NeurIPS*, volume 33, pp. 15920–15930, 2020.
- Chen, J., Cao, Z., Wang, J., Wu, Y., Qin, H., Zhang, Z., and Gong, Y.-J. Rethinking neural multi-objective combinatorial optimization via neat weight embedding. In *ICLR*, 2025a.
- Chen, X.-L., Mei, Y., and Zhang, M. Learning adaptive neighborhood search with dual operator selection for capacitated vehicle routing problem. In *Genetic and Evolutionary Computation Conference*, pp. 1108–1116. Association for Computing Machinery, 2025b.
- Chen, Y., Chen, R., Luo, F., and Wang, Z. Improving generalization of neural combinatorial optimization for vehicle routing problems via test-time projection learning. *arXiv preprint arXiv: 2506.02392*, 2025c.
- Drakulic, D., Michel, S., and Andreoli, J.-M. GOAL: A generalist combinatorial optimization agent learner. In *ICLR*, 2025.
- Fang, H., Song, Z., Weng, P., and Ban, Y. INViT: A generalizable routing problem solver with invariant nested view transformer. In *ICML*. JMLR, 2024.
- Feng, S., Lin, Z., Zhou, J., Zhang, C., Li, J., Chen, K.-W., Jayavelu, S., and Ong, Y.-S. Lifelong learner: Discovering versatile neural solvers for vehicle routing problems. *arXiv preprint arXiv: 2508.11679*, 2025.
- Gao, C., Shang, H., Xue, K., Li, D., and Qian, C. Towards generalizable neural solvers for vehicle routing problems via ensemble with transferrable local policy. In *International Joint Conference on Artificial Intelligence*, 2024.
- Guo, T., Mei, Y., Zhang, M., Zhao, H., Cai, K., and Du, W. Learning-aided neighborhood search for vehicle routing problems. *IEEE Transactions on Pattern Analysis and Machine Intelligence*, 47(7):5930–5944, 2025.
- Huang, Z., Zhou, J., Cao, Z., and Xu, Y. Rethinking light decoder-based solvers for vehicle routing problems. In *ICLR*, 2025.
- Isele, D. and Cosgun, A. Selective experience replay for lifelong learning. In *AAAI*, volume 32, 2018.
- Jiang, Y., Wu, Y., Cao, Z., and Zhang, J. Learning to solve routing problems via distributionally robust optimization. In *AAAI*, volume 36, pp. 9786–9794, 2022.
- Jiang, Y., Cao, Z., Wu, Y., Song, W., and Zhang, J. Ensemble-based deep reinforcement learning for vehicle routing problems under distribution shift. In *NeurIPS*, volume 36, pp. 53112–53125, 2023.
- Khetarpal, K., Riemer, M., Rish, I., and Precup, D. Towards continual reinforcement learning: A review and perspectives. *Journal of Artificial Intelligence Research*, 75:1401–1476, 2022.
- Kong, D., Ma, Y., Cao, Z., Yu, T., and Xiao, J. Efficient neural collaborative search for pickup and delivery problems. *IEEE Transactions on Pattern Analysis and Machine Intelligence*, 46(12):11019–11034, 2024.
- Kool, W., van Hoof, H., and Welling, M. Attention, learn to solve routing problems! In *ICLR*, 2019.
- Kwon, Y.-D., Choo, J., Kim, B., Yoon, I., Gwon, Y., and Min, S. Pomo: Policy optimization with multiple optima for reinforcement learning. In *NeurIPS*, volume 33, pp. 21188–21198, 2020.
- Li, J., Cao, Z., Wu, Y., and Liu, T. Enhancing the cross-size generalization for solving vehicle routing problems via continual learning. *arXiv preprint arXiv:2510.10262*, 2025a.
- Li, J., Li, H., and Zhao, X. Spatial–temporal evolution theory and influencing mechanisms of the express delivery network: A case on YTO express in China. *Transport Policy*, 171:408–424, 2025b.
- Lin, Z., Wu, Y., Zhou, B., Cao, Z., Song, W., Zhang, Y., and Jayavelu, S. Cross-problem learning for solving vehicle routing problems. In *International Joint Conference on Artificial Intelligence*, pp. 6958 – 6966, 2024.
- Liu, F., Lin, X., Liao, W., Wang, Z., Zhang, Q., Tong, X., and Yuan, M. Prompt learning for generalized vehicle routing. In *International Joint Conference on Artificial Intelligence*, pp. 6976–6984, 2024a.
- Liu, F., Lin, X., Wang, Z., Zhang, Q., Xialiang, T., and Yuan, M. Multi-task learning for routing problem with cross-problem zero-shot generalization. In *ACM SIGKDD Conference on Knowledge Discovery and Data Mining*, KDD, pp. 1898–1908, 2024b.

- Liu, J., Tang, K., and Yao, X. Robust optimization in uncertain capacitated arc routing problems: Progresses and perspectives. *IEEE Computational Intelligence Magazine*, 16(1):63–82, 2021.
- Liu, S., Zhang, Y., Tang, K., and Yao, X. How good is neural combinatorial optimization? A systematic evaluation on the traveling salesman problem. *IEEE Computational Intelligence Magazine*, 18(3):14–28, 2023.
- Luo, F., Wu, Y., Zheng, Z., and Wang, Z. Rethinking neural combinatorial optimization for vehicle routing problems with different constraint tightness degrees. *arXiv preprint arXiv: 2505.24627*, 2025.
- Ma, Y., Cao, Z., and Chee, Y. M. Learning to search feasible and infeasible regions of routing problems with flexible neural k-opt. In *NeurIPS*, volume 36, pp. 49555–49578, 2023.
- Mardešić, N., Erdelić, T., Carić, T., and Đurasević, M. Review of stochastic dynamic vehicle routing in the evolving urban logistics environment. *Mathematics*, 12(1), 2024.
- Markov, I., Bierlaire, M., Cordeau, J.-F., Maknoon, Y., and Varone, S. Waste collection inventory routing with non-stationary stochastic demands. *Computers & Operations Research*, 113:104798, 2020.
- Pan, W., Xiong, H., Ma, J., Zhao, W., Li, Y., and Yan, J. UniCO: On unified combinatorial optimization via problem reduction to matrix-encoded general TSP. In *ICLR*, 2025.
- Pei, J., Mei, Y., Liu, J., and Zhang, M. LiBOG: Lifelong learning for black-box optimizer generation. In *International Joint Conference on Artificial Intelligence*, pp. 8912–8920, 2025a.
- Pei, J., Mei, Y., Liu, J., Zhang, M., and Yao, X. Adaptive operator selection for meta-heuristics: A survey. *IEEE Transactions on Artificial Intelligence*, 6(8):1991–2012, 2025b.
- Pei, J., Mei, Y., Liu, J., Zhang, M., and Yao, X. Lifelong learning with behavior consolidation for vehicle routing. *arXiv preprint arXiv:2509.21765*, 2025c.
- Reinelt, G. TSPLIB—A traveling salesman problem library. *ORSA Journal on Computing*, 3(4):376–384, 1991.
- Rosin, C. D. and Belew, R. K. New methods for competitive coevolution. *Evolutionary Computation*, 5(1):1–29, 1997.
- Sun, R., Zheng, Z., and Wang, Z. Learning encodings for constructive neural combinatorial optimization needs to regret. In *AAAI*, volume 38, pp. 20803–20811, 2024.
- Sun, Y., Tang, K., Zhu, Z., and Yao, X. Concept drift adaptation by exploiting historical knowledge. *IEEE Transactions on Neural Networks and Learning Systems*, 29(10):4822–4832, 2018.
- Tang, K. and Yao, X. Learn to optimize – A brief overview. *National Science Review*, 11(8):nwae132, 2024.
- Uchoa, E., Pecin, D., Pessoa, A., Poggi, M., Vidal, T., and Subramanian, A. New benchmark instances for the capacitated vehicle routing problem. *European Journal of Operational Research*, 257(3):845–858, 2017.
- Vitter, J. S. Random sampling with a reservoir. *ACM Transactions on Mathematical Software*, 11(1):37–57, 1985.
- Wang, C., Yu, Z., McAleer, S., Yu, T., and Yang, Y. ASP: Learn a universal neural solver! *IEEE Transactions on Pattern Analysis and Machine Intelligence*, 46(6):4102–4114, 2024a.
- Wang, L., Zhang, X., Su, H., and Zhu, J. A comprehensive survey of continual learning: Theory, method and application. *IEEE Transactions on Pattern Analysis and Machine Intelligence*, 46(8):5362–5383, 2024b.
- Wang, S., Mei, Y., and Zhang, M. Explaining genetic programming-evolved routing policies for uncertain capacitated arc routing problems. *IEEE Transactions on Evolutionary Computation*, 28(4):918–932, 2024c.
- Wang, Y., Jia, Y.-H., Chen, W.-N., and Mei, Y. Distance-aware attention reshaping: Enhance generalization of neural solver for large-scale vehicle routing problems. *arXiv preprint arXiv: 2401.06979*, 2024d.
- Wu, Y., Song, W., Cao, Z., Zhang, J., and Lim, A. Learning improvement heuristics for solving routing problems. *IEEE Transactions on Neural Networks and Learning Systems*, 33(9):5057–5069, 2022.
- Xiao, Y., Wang, D., Wu, X., Wu, Y., Li, B., Du, W., Wang, L., and Zhou, Y. Improving generalization of neural vehicle routing problem solvers through the lens of model architecture. *Neural Networks*, 187:107380, 2025.
- Yang, S. Evolutionary computation for dynamic optimization problems. In *Annual Conference on Genetic and Evolutionary Computation*, pp. 629–649. Association for Computing Machinery, 2015.
- Zhang, S., Tino, P., and Yao, X. Hierarchical reduced-space drift detection framework for multivariate supervised data streams. *IEEE Transactions on Knowledge and Data Engineering*, 35(3):2628–2640, 2023.
- Zheng, Y., Luo, F., Wang, Z., Wu, Y., and Zhou, Y. MTL-KD: Multi-task learning via knowledge distillation for

generalizable neural vehicle routing solver. *arXiv preprint arXiv: 2506.02935*, 2025.

Zhou, C., Lin, X., Wang, Z., and Zhang, Q. Learning to reduce search space for generalizable neural routing solver. *arXiv preprint arXiv: 2503.03137*, 2025a.

Zhou, C., Yu, C., Yao, S., Lin, X., Wang, Z., Zhou, Y., and Zhang, Q. URS: A unified neural routing solver for cross-problem zero-shot generalization. *arXiv preprint arXiv: 2509.23413*, 2025b.

Zhou, J., Wu, Y., Song, W., Cao, Z., and Zhang, J. Towards omni-generalizable neural methods for vehicle routing problems. In *ICML*, volume 202, pp. 42769–42789. PMLR, 2023.

Zhou, J., Cao, Z., Wu, Y., Song, W., Ma, Y., Zhang, J., and Chi, X. MVMoE: Multi-task vehicle routing solver with mixture-of-experts. In *ICML*, volume 235, pp. 61804–61824. PMLR, 2024.

A. Details of DREE

A.1. General Process

Algorithm 1 demonstrates the process of DREE. For each learning time step (epoch), following common practice (Kwon et al., 2020; Zhou et al., 2023; Pei et al., 2025c), DREE iteratively learns in units of batch. In each iteration, a batch of new instances of the current task is sampled, obtaining \mathcal{L}_{DRL} to learn the current task. One experience batch is sampled, on which \mathcal{L}_{BR} is obtained to learn from buffered behavior. PIR is conditionally conducted based on N , to better balance between plasticity and stability. To calculate each loss term (i.e., \mathcal{L}_{DRL} , \mathcal{L}_{BR} , or \mathcal{L}_{PIR}) based on an instance/experience batch, DREE takes the average value over the batch.

Algorithm 1 DREE Lifelong Learning

```

1: Input:  $\{P_t\}_{t=1}^T, \theta_0$ 
2: Parameters:  $\alpha, \beta, \text{UB}, \text{LB}, |\mathcal{B}|$ 
3: Output:  $\theta$ 
4: Initialize buffer  $\mathcal{B} \leftarrow \emptyset$ 
5: for  $t \in \{1, \dots, T\}$  do
6:   for  $i \in \{1, \dots, I\}$  do
7:      $\{p\} \leftarrow$  a batch of  $M$  instances from  $P_t$ 
8:      $\{[s_\theta, \pi_\theta], f(\theta, p)\} \leftarrow$  Solve  $\{p\}$  with  $\theta$ 
9:      $\mathcal{L}_{\text{DRL}} \leftarrow$  base solver loss
10:    if  $\mathcal{B}$  is not empty then
11:       $\{e\} \leftarrow$  uniformly sample
12:       $\mathcal{L}_{\text{BR}} \leftarrow \text{BR}$ 
13:      if  $i - i' = N$  then
14:         $\mathcal{L}_{\text{PIR}}, M^+ \leftarrow \text{PIR}$ 
15:         $i' \leftarrow i$ 
16:         $N \leftarrow \text{UB} - \frac{M^+}{M} (\text{UB} - \text{LB})$ 
17:      else
18:         $\mathcal{L}_{\text{PIR}} \leftarrow 0$ 
19:      end if
20:    else
21:       $\mathcal{L}_{\text{PIR}} \leftarrow 0, \mathcal{L}_{\text{BR}} \leftarrow 0$ 
22:    end if
23:     $\mathcal{L} \leftarrow \mathcal{L}_{\text{DRL}} + \alpha \mathcal{L}_{\text{BR}} + \beta \mathcal{L}_{\text{PIR}}$ 
24:     $\theta \leftarrow \text{Optimize}(\theta, \mathcal{L})$ 
25:     $\mathcal{B} \leftarrow$  reservoir sampling ( $\{[s_\theta, \pi_\theta]\}\}, \mathcal{B}$ )
26:    update  $e$  with  $\{\langle p, f(\theta, p), [s_\theta, \pi_\theta] \rangle\}$  for any  $f(\theta, p) < f_b$ 
27:  end for
28: end for
29: return  $\theta$ 

```

A.2. Hyperparameters

DREE introduce five new hyperparameters, i.e., the coefficients of PIR and BR loss terms α and β , the buffer size $|\mathcal{B}|$, and the upper and lower bound of PIR interval UB and LB. We set $\alpha = 100$ as suggested in Pei et al. (2025c). Intuitively, we set $\beta = 1$ as PIR is analogous to training on new-task instance (obtaining \mathcal{L}_{DRL}).

The UB and LB determine the admissible range of N , thereby affecting the overall computational overhead of PIR throughout lifelong learning as well as the resulting plasticity–stability trade-off. In our implementation, we set this range heuristically to 1–4. As demonstrated in our experiments (cf. Section 5.4), DREE can automatically adapt its behavior, making its performance relatively insensitive to this choice.

$|\mathcal{B}|$ controls the buffer’s coverage of instances from previous tasks as well as the diversity of stored instances. Intuitively, a larger $|\mathcal{B}|$ can improve performance, but it also incurs higher storage cost. We set $|\mathcal{B}| = 256$ because it provides broad

coverage while maintaining acceptable storage overhead.

B. Setting Details

B.1. Dataset

The six principal tasks and the five orders follow exactly the experimental setting of [Pei et al. \(2025c\)](#). Problem scale and node coordinate distribution change between tasks for both CVRP and TSP. For CVRP, the node demand will also change. Notably, the coordinate of the depot for CVRP remains unchanged for all task.

We use an epoch as the time step unit. Drift occurs only between epochs, and the task is assumed stationary within each epoch. Since VRP instances are discrete and combinatorial, whose natural unit of change is a node, epoch-level granularity is sufficient for our continual drift design. Specifically, with principal problem scales of 20, 50, and 100 and 200 epochs between consecutive principal tasks, a change of one node in scale (or, equivalently, a one-node deviation from a principal distribution) corresponds to roughly two epochs. Hence, treating each epoch as a time step provides adequate resolution, and using finer-grained units would not significantly affect the outcomes. Following [Pei et al. \(2025c\)](#), we use representative subsets of TSPLIB and CVRPLIB (Set-X), as listed in Tables 8 and 9.

B.2. Training and Test Settings

Following [Pei et al. \(2025c\)](#), we assume the problem instance generation is uncontrollable. For all methods, during training, we use data augmentation with an augmentation factor of 8, following common settings ([Kwon et al., 2020](#); [Fang et al., 2024](#)). During testing, augmentation is not used.

With 1000 epochs and 128 batches per epoch, DREE with $|\mathcal{B}| = 256$ can retain only about 0.2% of the instances generated throughout lifelong learning. Nevertheless, given its strong performance, we consider this cost acceptable.

We conduct tests only on the six principal tasks. This choice is necessary because the intermediate tasks induced by continual drift can vary across different task orders, whereas the six principal tasks always appear regardless of the order. Testing these shared tasks therefore enables a fair and comprehensive comparison across orders. Since the principal tasks are uniformly distributed over the learning horizon, performance on them is also representative of overall lifelong-learning behavior. For testing, we report the optimality gap. For each test instance, we obtain an optimal solution using HGS for CVRP and Gurobi for TSP, compute the gap per instance, and then average gaps over the test set. All task orders share the same test-instance sets.

DREE trains on 128 batches of new-task instances per epoch. We record the number of PIR steps and find that, across different task orders, it is approximately 36 (avg. $N = \frac{128}{36} \simeq 3.56$). Therefore, for other methods (i.e., *fine-tuning*, LLR-BC, and *Li*), we run $128 + 36 = 164$ batches per epoch so that they execute the same number of solving episodes, while processing even more training instances. This ensures that DREE's performance gains are not attributable to longer training time or more training instances.

B.3. Adaption of Compared Methods

We implement the *intra* variant of *Li* ([Li et al., 2025a](#)) following the description in the original paper. Because, to the best of our knowledge, no official implementation is publicly available. To fit our scenario, where the generation of problem instances cannot be controlled, we maintain an instance buffer of size 256 that stores all observed instances via reservoir sampling, matching the design used in DREE. For *Li*, we set $\alpha = 0.5$, since the paper does not provide a recommended choice or selection guideline. We do not include the *inter* version of *Li* for the same reason as LiBOG ([Pei et al., 2025a](#)) and the method of [Feng et al. \(2025\)](#), i.e., it requires storing all models for all learned stationary tasks, comparing the current model against all stored models. In a continually drifting scenario, the number of potential stationary tasks can be very large, making the computational costs impractical.

LLR-BC buffers experiences only in the final epoch of each task ([Pei et al., 2025c](#)). As the task is different in the continually drifting scenario, we conduct buffering in each epoch. All other process and hyperparameter settings are identical to the description of [Pei et al. \(2025c\)](#).

C. Experiment Details

C.1. Performance on Seen Tasks

Table 6 and 7 list the detailed metric values of each method on each task order on CVRP and TSP, respectively.

Table 6. Detailed metric values on each task order of CVRP.

Order	Method	AP	AFB	AMFB	ABPI
1	Fine-tuning	14.05	10.35	21.85	3.7
	Li	6.12	0.07	0.07	6.06
	LLR-BC	4.5	1.03	1.99	3.48
	DREE	3.16	0.22	0.42	2.94
2	Fine-tuning	5.4	2.6	8.37	2.79
	Li	5.62	0.07	0.08	5.56
	LLR-BC	3.75	0.91	1.55	2.84
	DREE	3.21	0.5	1.03	2.71
3	Fine-tuning	14.17	10.93	18.93	3.25
	Li	6.21	0.02	0.03	6.19
	LLR-BC	4.32	1.35	1.74	2.97
	DREE	3.24	0.24	0.47	3
4	Fine-tuning	5.78	2.56	8.3	3.23
	Li	6.04	0.19	0.2	5.85
	LLR-BC	4.27	1.2	1.68	3.07
	DREE	2.87	0.1	0.1	2.77
5	Fine-tuning	4.34	0.91	21.28	3.43
	Li	6.8	0.12	0.12	6.69
	LLR-BC	4.13	0.71	1.45	3.42
	DREE	3.09	0.1	0.1	2.99

C.2. Generalisation on Unseen Benchmark Instances

We use the same representative instance sets as those selected in (Zhou et al., 2023; Pei et al., 2025c). Tables 8 and 9 report detailed test performance on CVRPLIB and TSPLIB instances, respectively. Gaps are computed based on the reported best-known solutions.

C.3. More Details of Applicability Experiment

Different Base Solver. We implement *fine-tuning*, the most widely used strategy, LLR-BC, the state-of-the-art lifelong learning solver, and DREE on another existing cross-distribution cross-scale neural solvers, INViT (Fang et al., 2024) and Omni (Zhou et al., 2023). We use 16 batches per epoch. It is smaller than the original setting of Fang et al. (2024), as lifelong learning is significantly more time-consuming than one-off training. We expect that with a longer budget, DREE can still outperform the compared lifelong learning solvers. Hyperparameters of lifelong learning methods are set identically to those used on POMO. Hyperparameters of base neural solvers are set identically to those in the original papers. Notably, we focus on comparing different lifelong learning solvers built upon the same base solver, rather than comparing across different base solvers. Results obtained with different base solvers are not directly comparable, since the training setups are different.

C.4. More Details of Ablation Study

The ablation variant *nPIR* sets \mathcal{L}_{PIR} to 0 for all epochs throughout lifelong learning. We still perform PIR so that EE can be executed. The ablation variant *nBR* removes the BR module from DREE. Consequently, EE no longer influences learning, since the enhanced behaviors are not used. The ablation variant *nEE* disables behavior replacement after PIR. This modification affects the BR module (as the quality of buffered behaviors is no longer improved) but does not impact the PIR

Table 7. Detailed metric values on each task order of TSP.

Order	Method	AP	AFB	AMFB	ABPI
1	Fine-tuning	1.86	0.75	1.59	1.11
	Li	3.64	0.01	0.01	3.63
	LLR-BC	1.1	0.1	0.1	1
	DREE	1.14	0.04	0.05	1.10
2	Fine-tuning	1.59	0.83	1.31	0.76
	Li	4.15	0.0	0.0	4.15
	LLR-BC	1.07	0.13	0.25	0.94
	DREE	1.13	0.14	0.15	0.99
3	Fine-tuning	1.8	0.92	1.29	0.88
	Li	3.34	0.01	0.02	3.33
	LLR-BC	1.15	0.11	0.24	1.05
	DREE	0.99	0.04	0.05	0.94
4	Fine-tuning	2.16	0.96	1.96	1.2
	Li	5.09	0.02	0.12	5.07
	LLR-BC	1.62	0.31	0.65	1.31
	DREE	1.09	0.02	0.03	1.08
5	Fine-tuning	2.44	0.86	2.06	1.58
	Li	5.95	0.03	0.11	5.92
	LLR-BC	1.87	0.2	0.37	1.67
	DREE	1.73	0.04	0.09	1.68

module. For all ablation variants, we fix $N \leftarrow 3.56$. Because different ablations have different learning capacities, they may converge to different expected values of M^+ . Fixing N ensures that all ablation variants perform the same number of PIR executions, enabling a fairer comparison.

C.5. More Details of Hyperparameter Analysis

Notably, a larger $|\mathcal{B}|$ and a smaller N (with its range defined by UB and LB) intuitively incur higher computational cost and may yield better performance. Therefore, we only evaluate the lower-cost variants, in which $|\mathcal{B}|$ is smaller, UB is larger, or LB is larger.

As the results listed in Table 5 show, different hyperparameter settings lead to different performance. Arguably, $\beta(2)$ and $\alpha(50)$ are the best tested settings for CVRP and TSP, respectively. However, compared with the performance of existing methods (cf. Table 1), the performance changes due to different hyperparameter settings are slight, indicating the hyperparameter robustness of DREE.

Table 8. Test results on each included CVRPLIB instance.

Instance	Multi-task		Fine-tuning		Li		LLR-BC		DREE	
	Distance	Gap (%)	Distance	Gap (%)	Distance	Gap (%)	Distance	Gap (%)	Distance	Gap (%)
X-n1001-k43	86266.88	19.23	90196.17	24.66	91417.62	26.35	94755.37	30.96	89635.44	23.88
X-n101-k25	29988.91	8.69	30540.37	10.69	30926.36	12.09	29478.07	6.84	29539.54	7.06
X-n153-k22	24036.21	13.27	24083.69	13.5	25059.6	18.09	24751.04	16.64	23686.61	11.62
X-n200-k36	62479.91	6.66	62848.84	7.29	65328.33	11.52	62325.69	6.4	62200.68	6.18
X-n251-k28	41563.26	7.44	42712.81	10.41	43884.06	13.44	44103.78	14.01	41718.06	7.84
X-n303-k21	24117.38	10.96	26153.8	20.32	27413.56	26.12	25996.89	19.6	24596.6	13.16
X-n351-k40	29544.25	14.09	30682.58	18.48	32419.11	25.19	33240.53	28.36	29324.47	13.24
X-n401-k29	70920.75	7.21	71970.64	8.79	77196.08	16.69	81340.6	22.96	70874.54	7.14
X-n459-k26	28831.45	19.44	30027.02	24.39	32952.42	36.51	30024.71	24.38	28680.1	18.81
X-n502-k39	75043.78	8.4	74583.1	7.74	77735.05	12.29	84633.9	22.26	73331.75	5.93
X-n548-k50	95298.19	9.92	96827.34	11.68	101873.6	17.5	112970.4	30.3	95291.28	9.91
X-n599-k92	121070.5	11.64	125330.2	15.56	138531.8	27.74	132365.1	22.05	121676.1	12.19
X-n655-k131	118827	11.28	115713.6	8.37	124589	16.68	145577.2	36.33	115984.8	8.62
X-n701-k44	93125.35	13.67	96309.91	17.56	95707.08	16.83	96237.26	17.47	92692.63	13.15
X-n749-k98	87428.02	13.15	91824.92	18.84	100277.4	29.78	100074	29.51	89567.84	15.92
X-n801-k40	85760.6	16.98	87867.68	19.86	89375.21	21.91	179235.1	144.49	84788.5	15.66
X-n856-k95	99516.53	11.86	107203	20.5	110038.4	23.69	151211.4	69.97	105347.8	18.41
X-n895-k37	68330.28	26.87	69874.6	29.73	70757.8	31.37	97394.1	80.83	67637.25	25.58
X-n957-k87	97976.01	14.64	104127.2	21.84	109240.4	27.82	130347.2	52.52	108971.7	27.5

Table 9. Test results on each included TSPLIB instance.

Instance	Multi-task		Fine-tuning		Li		LLR-BC		DREE	
	Distance	Gap (%)	Distance	Gap (%)	Distance	Gap (%)	Distance	Gap (%)	Distance	Gap (%)
a280	3042.01	17.95	3067.16	18.93	3360.59	30.31	3083.86	19.58	3068.86	18.99
d493	51872.83	48.2	48369.09	38.19	55392.14	58.25	48178.12	37.64	47438.62	35.53
d657	63991.38	30.83	64949.99	32.79	69454.31	42	63407.77	29.64	63573.1	29.97
fl417	13726.64	15.73	13643.5	15.03	13696.16	15.47	13708.06	15.57	13509.45	13.9
kroA100	22350.05	5.02	22719.97	6.76	24029.82	12.91	22620	6.29	22495.75	5.7
kroA150	28621.91	7.91	28467.85	7.33	30349.84	14.42	28544.16	7.62	28068.52	5.82
kroA200	32378.11	10.25	32931.33	12.13	34288.3	16.75	32319.52	10.05	32258.52	9.84
kroB200	33546.88	13.96	33121.93	12.52	35114.09	19.29	32903.38	11.78	32939.82	11.9
lin318	49056.6	16.72	49268.01	17.22	52593.37	25.14	49458.64	17.68	49158.75	16.96
p654	42974.79	24.05	41371.89	19.42	45467.48	31.25	41185.71	18.89	41484.49	19.75
pcb442	61088.63	20.31	61423.84	20.97	69073.19	36.03	62534.2	23.15	61799.27	21.7
pr1002	353243.6	36.36	347019.3	33.96	390824.7	50.87	355881.1	37.38	351847.6	35.82
pr226	83418.01	3.79	83694.54	4.14	86377.18	7.48	84369.12	4.98	84224.02	4.8
pr264	54771.85	11.47	53165.7	8.2	62884.41	27.98	52411.08	6.67	53920.21	9.74
pr299	57926.24	20.2	58615.6	21.63	62212.08	29.09	56126.65	16.47	57072.41	18.43
pr439	134547.6	25.49	133522.1	24.53	147491.2	37.56	131621.3	22.76	134193.3	25.16
rat575	8550.87	26.25	8479.65	25.2	9702.2	43.25	8574.6	26.6	8503.19	25.55
rat783	11577.88	31.48	11608.1	31.82	13347.75	51.58	11487.35	30.45	11583.39	31.54
rd400	18396.2	20.39	18363.85	20.17	19687.65	28.84	18278.13	19.61	18395.16	20.38
ts225	134234.4	5.99	137818.5	8.82	146137.8	15.39	137053.6	8.22	135116.3	6.69
tsp225	4360.97	11.36	4492.83	14.73	4593.41	17.3	4406.61	12.53	4335.81	10.72
u574	46249.28	25.32	48140.74	30.45	51238.19	38.84	45324.73	22.81	46205.06	25.2
u724	53539.75	27.75	54104.91	29.1	60594.15	44.58	53929.43	28.68	53489.39	27.63